Extra fermions in E_6 superstring theories

V. Barger
Physics Department, University of Wisconsin, Madison, Wisconsin 53706

N. G. Deshpande
Institute of Theoretical Science, University of Oregon, Eugene, Oregon 97403

R. J. N. Phillips
Rutherford Appleton Laboratory, Chilton, Didcot, Oxon, England

K. Whisnant
Physics Department, Florida State University, Tallahassee, Florida 32306
(Received 4 December 1985)

In E_6 superstring theories, there are new fermion fields which lie in the 27-dimensional representation along with the known fermions. We examine possible production modes of these exotic fermions and their likely decays. Whereas e^+e^- collider data exclude new charged fermions with masses below 23 GeV, it appears that present $p\bar{p}$ collider data for dimuons and for isolated single electrons exclude exotic quarks with masses below 30 GeV and considerable regions of lepton mass assignments in the range 20—45 GeV (assuming $m_E > m_{\nu_E}, m_{N_E}$). We place constraints on the mixings of the exotic fermions from experimental limits on flavor-changing neutral currents and the observed weak universality of charged-current interactions. The decays of the exotic h quark (singlet, charge $-\frac{1}{3}$) satisfy the bound $\Gamma(h\to de^+e^-)/\Gamma(h\to ue\nu)\gtrsim 12\%$. Production and decays of very heavy exotics are also considered.

I. INTRODUCTION

In superstring theories with an E_6 gauge group remaining after compactification[1-5] the fermions lie in three or more 27 representations which contain extra fermion fields.[6,7] In addition to known fermions, each 27 has a charge $-\frac{1}{3}$ quark singlet h, lepton doublets $(\nu_E, E^-)_L$ and $(N_E, E^-)_R$, and neutral-lepton singlets N_R, n_L. Mixing of exotics with known fermions determine to a considerable extent the production and decay systematics of the exotics. One important consequence of the mixing is flavor-changing neutral-current (FCNC) couplings;[8,9] the decays of the exotic h quark (singlet, charge $-\frac{1}{3}$) satisfy the bound $\Gamma(h\to de^+e^-)/\Gamma(h\to ue\nu)\gtrsim 12\%$. We explore the consequences for the decay and the detection of exotic E_6 fermions, and compare illustrative calculations with present experimental data. Significant limits on exotic-fermion masses come not only from e^+e^- collider data, but also from dimuon and isolated-electron measurements at the CERN $p\bar{p}$ collider. Limits are also placed on the flavor-changing transitions from the processes (i) $K_L, K_S\to\mu^+\mu^-$, (ii) K^0-$\bar{K}^0$ mixing, (iii) $b\to q\mu^+\mu^-$, and (iv) $\mu\to 3e$, $\tau\to 3e, 3\mu$.

A state in E_6 can be specified by its color charge under SU(3) and the quantum numbers $Q, I_{3L}, \tilde{Q}, I_{3R}$, where Q, I_{3L} are the usual charge and weak isospin and $\tilde{Q}, I_{3R}$ are proportional to the hypercharges of two additional U(1) groups. The fermion assignments in the 27 representation are given in Table I. For just one extra U(1) group, the additional Z boson couples to the charge $\tilde{Q}$.

For the minimal rank-5 superstring model of E_6, we can write the neutral-current (NC) part of the Lagrangian as[10,11]

$$\mathcal{L}_{\rm NC} = eA_\mu J^\mu_{\rm EM} + g_Z Z_\mu J^\mu_Z + g' Z'_\mu J^\mu_{Z'} , \tag{1}$$

where $J^\mu_{\rm EM}$ and J^μ_Z ($\equiv J^\mu_3 - x_W J^\mu_{\rm EM}$) are the usual electromagnetic and Z-boson currents and

$$J^\mu_{Z'} = 2\bar{f}_L\gamma^\mu\tilde{Q}f_L + 2\bar{f}_R\gamma^\mu\tilde{Q}f_R . \tag{2}$$

The coupling constants g' and g_Z are given by

$$g' = \frac{e}{\sqrt{1-x_W}}, \quad g_Z = \frac{e}{\sqrt{x_W}\sqrt{1-x_W}} , \tag{3}$$

where $x_W = \sin^2\theta_W$. The low-energy effective Lagrangian is

$$\mathcal{L}_{\rm eff} = \frac{4G_f}{\sqrt{2}}[\rho_1{}^2 J_Z{}^2 + (\rho_2 J_Z + \eta J_{Z'})^2] . \tag{4}$$

In superstring theories only $SU(2)_L$-doublet and -singlet Higgs bosons contribute to gauge-boson masses so that $\rho_1 \equiv 1$. It has been shown[11] that low-energy neutral-current phenomenology and the W and Z mass measurements constrain the parameters to $x_W = 0.222^{+0.017}_{-0.013}$, $\rho_2 = 0.08^{+0.07}_{-0.16}$, and $\eta = 0.26^{+0.22}_{-0.26}$. Thus to a good approximation we can ignore ρ_2 in the present analysis. Then the only unknown is the Z' mass which is constrained to be above 107 GeV (143 GeV) if its decays to exotic fermions are kinematically allowed (suppressed).

The presence of additional quarks and leptons in 27

TABLE I. Decomposition of 27 and fermion quantum numbers.

SO(10)	SU(5)	Left-handed state	SU(3)	Q	I_{3L}	$\tilde{Q}$	I_{3R}
16	5*	d^c	3*	$\frac{1}{3}$	0	$-\frac{1}{6}$	$\frac{1}{2}$
		e^-	1	-1	$-\frac{1}{2}$	$-\frac{1}{6}$	0
		ν_e	1	0	$\frac{1}{2}$	$-\frac{1}{6}$	0
	10	e^{-c}	1	1	0	$\frac{1}{3}$	$\frac{1}{2}$
		d	3	$-\frac{1}{3}$	$-\frac{1}{2}$	$\frac{1}{3}$	0
		u	3	$\frac{2}{3}$	$\frac{1}{2}$	$\frac{1}{3}$	0
		u^c	3*	$-\frac{2}{3}$	0	$\frac{1}{3}$	$-\frac{1}{2}$
	1	N^c	1	0	0	$\frac{5}{6}$	$-\frac{1}{2}$
10	5*	h^c	3*	$\frac{1}{3}$	0	$-\frac{1}{6}$	0
		E^-	1	-1	$-\frac{1}{2}$	$-\frac{1}{6}$	$-\frac{1}{2}$
		ν_E	1	0	$\frac{1}{2}$	$-\frac{1}{6}$	$-\frac{1}{2}$
	5	h	3	$-\frac{1}{3}$	0	$-\frac{2}{3}$	0
		E^{-c}	1	1	$\frac{1}{2}$	$-\frac{2}{3}$	$\frac{1}{2}$
		N_E^c	1	0	$-\frac{1}{2}$	$-\frac{2}{3}$	$\frac{1}{2}$
1	1	n	1	0	0	$\frac{5}{6}$	0

representations causes not only flavor-changing neutral currents but also possible deviations from weak universality in charged-current processes. This follows from the fact that the Weinberg-Glashow-Paschos condition[12] for flavor conservation—all fermions with the same charge and helicity have the same SU(2) quantum numbers—is not obeyed any longer. The mass matrices that are responsible for the mixing depend in general on arbitrary Yukawa couplings as well as expectation values of various Higgs fields. [There are five vacuum expectation values (VEV's) in each 27 representation of Higgs fields.] In string theories the Yukawa couplings do not have any residual E_6 symmetry because the low-energy multiplets of fermions are arbitrary linear combinations of multiplets at the unification scale. Thus any quantitative estimate is unreliable. If it is assumed that all Yukawa couplings in one generation are of the same order of magnitude, and different mass scales arise from differences in VEV's of doublet and singlet Higgs bosons, then one possible qualitative solution is a d_L-h_L mixing angle $\alpha_h \sim m_d/m_h$ and a e_R-E_R mixing angle $\beta_E \sim m_e/m_E$. Weak universality then requires that the e_L-E_L and ν_e-ν_E mixing angles α_E and α_ν be close to each other. Because of theoretical uncertainties we do not pursue such an approach here. We shall treat mixing angles and masses as phenomenological parameters. Two types of FCNC can occur in the gauge sector of E-e. First, there are exotic-nonexotic mixing currents (e.g., d-h or E-e) which are proportional to one power of a mixing angle (in the limit of small mixing between standard and exotic fermions); second, there are terms proportional to two powers of a mixing angle which give rise to FCNC among the standard quarks and leptons (and separately among the exotics). The first kind of FCNC will be relevant for single production of exotic fermions and their decays, whereas the second will lead to rare decays such as $K_L \to \mu\bar{\mu}$, $\mu \to e\bar{e}e$, and to K^0-$\bar{K}^0$ mixing. We shall obtain bounds on the latter processes relevant to E_6 theories.

The outline of the paper is as follows. In Sec. II the decays of the first generation exotic fermions are analyzed, under the simplifying assumption that mixings occur only within a given generation. The decay modes are illustrated in Fig. 1, where the W,Z may be either virtual or real.

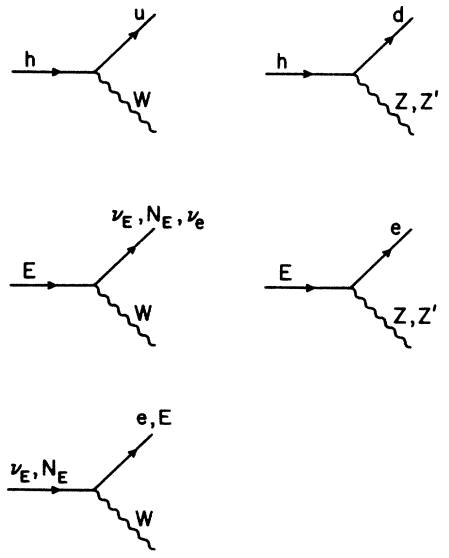

FIG. 1. Diagrams for exotic-fermion decays; final-state W,Z bosons may be virtual or real, depending on the exotic-fermion masses.

In Sec. III the production of exotic fermions at current and future e^+e^- colliders is addressed. Limits on the masses of neutral exotic leptons are discussed. Experimental signatures of the production of exotic fermions at the Z resonance energy are detailed. Section IV considers signatures at $p\bar{p}$ colliders. Dimuon and isolated-single-electron data from the CERN $p\bar{p}$ collider are used to place improved lower bounds on the masses of the h quark and exotic leptons. The production and decays of very heavy exotics are also considered. A discussion of mixing angle constraints from FCNC is given in Sec. V; constraints from weak universality of charged-current interactions are obtained in Sec. VI. A summary is given in Sec. VII.

II. EXOTIC-FERMION DECAYS

For simplicity, we assume mixing in the first generation only. Because the h quark is an $SU(2)_L$ singlet, it can decay only through mixing with the d quark, both by charged currents and neutral currents. Assuming h_L-d_L mixing is described by an angle α_h, the neutral-current decay rates are readily calculable using Eq. (1). The Lagrangian for h decays is (ignoring Kobayashi-Maskawa mixing)

$$\mathcal{L} = \sin\alpha_h \frac{g_L}{2\sqrt{2}} W_\mu^+ \bar{u}\gamma^\mu(1-\gamma_5)h - \sin\alpha_h \cos\alpha_h (\tfrac{1}{4}g_Z Z_\mu - \tfrac{1}{2}g' Z'_\mu) \times \bar{d}\gamma^\mu(1-\gamma_5)h + \text{H.c.} , \tag{5}$$

where $g_L = e/\sqrt{x_W}$. We consider here the case where h is sufficiently light that virtual W and Z propagator effects can be neglected. Defining $\Gamma_0^h = G_F^2 m_h^5/192\pi^3$, the h partial rates in the massless approximation for final-state particles are

$$\Gamma(h\to q_1\bar{q}_2 q_3) = \tfrac{1}{4}\Gamma_0^h(|a+c|^2+2|a|^2+2|c|^2+3|b|^2)\sin^2\alpha_h\cos^2\alpha_h ,$$
$$\Gamma(h\to q_1\bar{q}_1 q_1) = \tfrac{1}{4}\Gamma_0^h(4|a|^2+3|b|^2)\sin^2\alpha_h\cos^2\alpha_h, \quad \Gamma(h\to q l_1 \bar{l}_2) = \tfrac{1}{4}\Gamma_0^h(|a|^2+|b|^2)\sin^2\alpha_h\cos^2\alpha_h , \tag{6}$$

where a, b, and c are given in Table II. Neglecting $h\to tX$, the h lifetime is

$$\tau_h = \frac{8\times10^{-19}\ \text{sec}}{\sin^2\alpha_h\cos^2\alpha_h}\left[\frac{20\ \text{GeV}}{m_h}\right]^5 . \tag{7}$$

There is a small possibility that the h could travel a measurable distance before decaying, if $\alpha_h \lesssim m_d/m_h$. For $\sin^2\alpha_h \ll 1$, as would be expected from decay tests of weak universality, the branching fractions for the leading modes are

$$B(h\to\text{hadrons})\simeq 66\%, \quad B(h\to u l\bar{\nu}_l)\simeq 8\% ,$$
$$B(h\to d\nu_l\bar{\nu}_l)\simeq 2\%, \quad B(h\to d l\bar{l})\simeq 1\% , \tag{8}$$

where $l = e,\mu,\tau$. The contributions from the Z' do not affect these results significantly. These branching ratios will be reduced to some extent if final states with exotics are kinematically accessible.

The dilepton-to-lepton ratio in h decays is

$$r \equiv \frac{\Gamma(h_i\to l\bar{l}X)}{\Gamma(h_i\to l\bar{\nu}X)} = \tfrac{1}{4}[(-1+2x_W+\tfrac{2}{3}\eta^2)^2+(2x_W+\tfrac{4}{3}\eta^2)^2]\cos^2\alpha_h . \tag{9a}$$

From the limits on η from neutral-current data this ratio for small α_h must lie in the range

$$0.12 \le r \le 0.18 . \tag{9b}$$

The lower bound on this ratio is the same as that for b decays in a model without a top quark.[13,14]

For exotic-lepton decays, the mixing can, in general, be quite complicated. As in the discussion of h decays, we consider only mixing within the first generation and further assume that the dominant mixing in the neutral-lepton sector is between ν_e and ν_E and that the mixing angles between ν_e and N_E, N, n can be neglected here.[6] (Note, however, that these angles determine the decay rates for N,n.) Describing the e_L-E_L mixing by the angle α_E, the e_R-E_R mixing by the angle β_E and the ν_e-ν_E mixing by the angle α_ν, the Lagrangian for exotic-lepton decays is

$$\mathcal{L} = \frac{g_L}{2\sqrt{2}} W_\mu^+ \{ [\bar{e}\gamma^\mu(1-\gamma_5)\nu_e + \bar{E}\gamma^\mu(1-\gamma_5)\nu_E]\cos(\alpha_E-\alpha_\nu) + [\bar{E}\gamma^\mu(1-\gamma_5)\nu_e - \bar{e}\gamma^\mu(1-\gamma_5)\nu_E]\sin(\alpha_E-\alpha_\nu) + (-\sin\alpha_E\bar{e}+\cos\alpha_E\bar{E})\gamma^\mu(1+\gamma_5)N_E\} + \sin\beta_E\cos\beta_E(\tfrac{1}{4}g_Z Z_\mu - \tfrac{1}{2}g' Z'_\mu)\bar{e}\gamma^\mu(1+\gamma_5)E + \text{H.c.} \tag{10}$$

TABLE II. Coefficients for h decays in Eq. (6); mixings among final-state decay particles are neglected.

Decay	a	b	c
$h\to u(l\bar{\nu},s\bar{c})$	0	0	$2/\cos\alpha_h$
$h\to d\nu\bar{\nu}$	$1+\frac{2}{3}\eta^2$	0	0
$h\to dl\bar{l}$	$-1+2x_W+\frac{2}{3}\eta^2$	$2x_W+\frac{4}{3}\eta^2$	0
$h\to d(d\bar{d},s\bar{s},b\bar{b})$	$-1+\frac{2}{3}x_W-\frac{4}{3}\eta^2$	$\frac{2}{3}x_W-\frac{2}{3}\eta^2$	0
$h\to du\bar{u}$	$1-\frac{4}{3}x_W-\frac{4}{3}\eta^2$	$-\frac{4}{3}x_W+\frac{4}{3}\eta^2$	$-2/\cos\alpha_h$
$h\to dc\bar{c}$	$1-\frac{4}{3}x_W-\frac{4}{3}\eta^2$	$-\frac{4}{3}x_W+\frac{4}{3}\eta^2$	0

We distinguish two cases: scenario A with $m_E>m_{\nu_E},m_{N_E}$ and scenario B with $m_E<m_{\nu_E},m_{N_E}$.

Scenario A. The exotic charged lepton E will decay predominantly into $E\to\nu_E f_1\bar{f}_2, N_E f_1\bar{f}_2$ via unsuppressed charged-current interactions if kinematically allowed. The E lifetime is then approximately given by

$$\tau_E=\frac{10^{-18}\text{ sec}}{f(m_{\nu_E}{}^2/m_E{}^2)+f(m_{N_E}{}^2/m_E{}^2)}\left[\frac{20\text{ GeV}}{m_E}\right]^5, \quad (11)$$

where all known fermion masses are ignored (except for the t quark, which we assume to be heavy) and $f(x)=1-8x+8x^3-x^4+12x^2\ln x$. Branching fractions of the leading modes are

$$B(E\to\nu_E+\text{hadrons})+B(E\to N_E+\text{hadrons})\approx 66\%\ ,$$
$$B(E\to\nu_E e\bar{\nu}_e)+B(E\to N_E e\bar{\nu}_e)\approx 11\%\ . \quad (12)$$

The ν_E decays via $\nu_E\to e f_1\bar{f}_2$ with its decay rate suppressed by mixing. The ν_E lifetime and branching fractions depend crucially on its mass. For m_{ν_E} just below (significantly above) the τ mass the branching ratios are

$$B(\nu_E\to e\nu_e\bar{e})=B(\nu_E\to e\nu_\mu\bar{\mu})=20\%\ (11\%)\ ,$$
$$B(\nu_E\to e+\text{hadrons})=60\%\ (67\%)\ . \quad (13)$$

If $m_{\nu_E}<m_\pi$, then ν_E decays entirely through leptonic modes. The N_E branching fractions would be similar to those for ν_E.

Scenario B. The neutral leptons ν_E, N_E decay predominantly into $E+$virtual W. The ν_E lifetime formula is analogous to Eq. (11), with only one factor $f(m_E{}^2/m_{\nu_E}{}^2)$. The numerical values of the hadronic and leptonic branching fractions are the same as those in Eq. (12).

The decays of E occur through both charged and neutral currents. From Eq. (10) the partial rates in the approximation of massless final-state particles are

$$\Gamma(E\to ef\bar{f})=\Gamma_0^E\sin^2\beta_E\cos^2\beta_E\tfrac{1}{4}(|a|^2+|b|^2+|c|^2)c_f,\quad f\neq e\ , \quad (14)$$
$$\Gamma(E\to ee\bar{e})=\Gamma_0^E\sin^2\beta_E\cos^2\beta_E\tfrac{1}{4}(|a|^2+2|b|^2),\quad f=e\ ,$$

where $c_f=1$ for leptons and $c_f=3$ for quarks and $\Gamma_0^E=G_F{}^2m_E{}^5/192\pi^3$; the a, b, and c are given in Table III. For $\sin^2\beta_E\ll 1$ and $\sin^2(\alpha_E-\alpha_\nu)\ll 1$, the branching fractions for the leading decay modes are

$$\begin{aligned}
&B(E\to\nu_e+\text{hadrons})=47\%\ ,\\
&B(E\to e+\text{hadrons})=20\%\ ,\\
&B(E\to\nu_e\mu\bar{\nu}_\mu)\simeq B(E\to\nu_e\tau\bar{\nu}_\tau)\simeq 8\%\ ,\\
&B(E\to\nu_e e\bar{\nu}_e)\simeq 10\%\ ,\\
&B(E\to e\nu_\mu\bar{\nu}_\mu)\simeq B(E\to e\nu_\tau\bar{\nu}_\tau)\simeq 2\%\ ,\\
&B(E\to ee\bar{e})\simeq 10002\ ,\\
&B(E\to e\mu\bar{\mu})=B(E\to e\tau\bar{\tau})\simeq 1\%\ .
\end{aligned} \quad (15)$$

TABLE III. Coefficients for E decays in Eq. (14); mixings among final-state decay particles are neglected.

Decay	a	b	c
$E\to\nu_e(d\bar{u},s\bar{c},\mu\bar{\nu}_\mu,\tau\bar{\nu}_\tau)$	0	0	$\frac{2\sin(\alpha_E-\alpha_\nu)}{\sin\beta_E\cos\beta_E}$
$E\to e(\nu_\mu\bar{\nu}_\mu,\nu_\tau\bar{\nu}_\tau)$	$1+\frac{2}{3}\eta^2$	0	0
$E\to el\bar{l}$	$-1+2x_W+\frac{2}{3}\eta^2$	$2x_W+\frac{4}{3}\eta^2$	0
$E\to e(d\bar{d},s\bar{s},b\bar{b})$	$-1+\frac{2}{3}x_W-\frac{4}{3}\eta^2$	$\frac{2}{3}x_W-\frac{2}{3}\eta^2$	0
$E\to e(u\bar{u},c\bar{c})$	$1-\frac{4}{3}x_W-\frac{4}{3}\eta^2$	$-\frac{4}{3}x_W+\frac{4}{3}\eta^2$	0
$E\to e\nu_e\bar{\nu}_e$	$1+\frac{2}{3}\eta^2$	0	$\frac{2\sin(\alpha_E-\alpha_\nu)}{\sin\beta_E\cos\beta_E}$

Again, the Z' contributions do not affect these much. Note that there are substantial FCNC branching fractions.

III. PRODUCTION OF EXOTICS IN e^+e^- COLLISIONS

The charged exotics can be produced in pairs through the virtual photon and the Z boson; current limits from the DESY e^+e^- storage ring PETRA are $m_E > 23$ GeV and $m_h > 23$ GeV. On the Z resonance, pair production occurs in Z decay with partial rates[11]

$$\Gamma(Z\to E\bar{E}) = (0.11\text{ GeV})\left[1-\frac{4m_E^2}{m_Z^2}\right]^{1/2}\left[1+\frac{2m_E^2}{m_Z^2}\right], \quad (16a)$$

$$\Gamma(Z\to h\bar{h}) = (0.02\text{ GeV})\left[1-\frac{4m_h^2}{m_Z^2}\right]^{1/2}\left[1+\frac{2m_h^2}{m_Z^2}\right]. \quad (16b)$$

The exotics can also be produced singly[8] via mixing with light fermions in $Z\to e\bar{E}+\bar{E}e, h\bar{d}+\bar{d}h$. The partial rates for these decays are

$$\Gamma(Z\to e\bar{E}+\bar{E}e) = (0.36\text{ GeV})\sin^2\beta_E\cos^2\beta_E\left[1-\frac{m_E^2}{m_Z^2}\right]^2\left[1+\frac{m_E^2}{2m_Z^2}\right], \quad (17a)$$

$$\Gamma(Z\to h\bar{d}+\bar{d}h) = (1.08\text{ GeV})\sin^2\alpha_h\cos^2\alpha_h\left[1-\frac{m_h^2}{m_Z^2}\right]^2\left[1+\frac{m_h^2}{2m_Z^2}\right], \quad (17b)$$

where β_E is the e_R, E_R mixing angle. The primary electron or d-quark jet from the decays in Eq. (17b) can be "isolated" and energetic, with $E=(m_Z^2-m^2)/2m_Z$ where m is the exotic mass.

The subsequent muonic decay modes $E\to\nu_E\mu\bar{\nu}_\mu$, $N_E\mu\bar{\nu}_\mu$ occur about 11% of the time and lead to $\mu\bar{e}$ or $e\bar{\mu}$ events. If the decay products of the ν_E or N_E are observed, then the final states from E production can contain up to six charged leptons. In h decays, $h\to d\nu\bar{\nu}$ about 6% of the time, leading to events with missing energy. The mode $h\to d\mu\bar{\mu}$ leads to events with dimuons in about 1% of h decays.

Limits on the ν_E mass depend on the size of the mixing with ν_e. Decays of π, K, and D give the restriction[15] $|\sin(\alpha_\nu-\alpha_E)| \lesssim 10^{-3}$ for 10 MeV $\lesssim m_{\nu_E} \lesssim 1.5$ GeV. Single production of ν_E occurs through W exchange with cross section

$$\frac{\sigma(e^+e^-\to\nu_E\bar{\nu}_e)}{\sigma(e^+e^-\to\mu\bar{\mu})_{\rm QED}} = \sin^2(\alpha_\nu-\alpha_E)\frac{s^2}{m_W^4}\frac{1}{16x_W^2}\left[1-\frac{m_{\nu_E}^2}{s}\right]^2\times\left[1+\frac{m_{\nu_E}^2}{2s}\right]. \quad (18)$$

The hadronic decay of the ν_E would give monojet events[16] if m_{ν_E} is not too large. Limits from the SLAC e^+e^- storage ring PEP on monojet events[15,17] give the constraint $|\sin(\alpha_\nu-\alpha_E)| \lesssim 0.05$ for 2 GeV $\lesssim m_{\nu_E} \lesssim 12$ GeV.

For the reaction $e^+e^-\to\nu_E\bar{\nu}_E$ below the Z resonance, secondary vertex searches at PEP (Ref. 18) give some limits on $\sin(\alpha_\nu-\alpha_E)$ for ν_E masses up to $m_{\nu_E}=14$ GeV. The cross section is

$$\frac{\sigma(e^+e^-\to\nu_E\bar{\nu}_E)}{\sigma(e^+e^-\to\mu\bar{\mu})_{\rm QED}} = \frac{1+(1-4x_W)^2}{128x_W^2(1-x_W)^2}\frac{s^2}{(s-m_Z^2)^2+m_Z^2\Gamma_Z^2}\left[1-\frac{4m_{\nu_E}^2}{s}\right]^{1/2}\left[1-\frac{m_{\nu_E}^2}{s}\right], \quad (19)$$

which is unsuppressed by mixing angles. Results for N_E are similar to those for ν_E, except that $\alpha_E-\alpha_\nu$ is replaced by α_E and $1+m_{\nu_E}^2/2s$ in Eq. (18) is replaced by 3.

On the Z resonance the decay width to neutral-lepton pairs is

$$\Gamma(Z\to\nu_E\bar{\nu}_E)=\Gamma(Z\to N_E\bar{N}_E) = (0.18\text{ GeV})\left[1-\frac{4m_{\nu_E}^2}{m_Z^2}\right]^{1/2}\left[1-\frac{m_{\nu_E}^2}{m_Z^2}\right]. \quad (20)$$

The signature[19] is back-to-back decay cones possibly separated by gaps from the production vertex or one such cone with missing momentum if one of the neutral leptons decays outside the detector.

If the ν_E or N_E lifetime is too short to leave a gap, the decays $\nu_E, N_E\to e\bar{\mu}\nu_\mu$ will provide a distinctive signature. Because the V,A structure of the ν_E and N_E interaction differs, the two may be distinguished by energy, mass, or angular distributions, particularly if these exotic particles are heavy. Representative predicted distributions for neutral-lepton masses of 35 GeV are shown in Fig. 2.

The n,N leptons essentially decouple from the usual W and Z, but could be produced via the Z' boson. Their decays proceed through smaller mixing angles, which have been ignored in the discussion above.

IV. PRODUCTION OF EXOTICS IN $p\bar{p}$ COLLISIONS

The most promising place to look for evidence of the exotic leptons E,ν_E,N_E of each E_6 generation is in the decay of W and Z bosons,[11] provided their masses are low enough. At future $e^+e^-\to Z^0$ factories, the

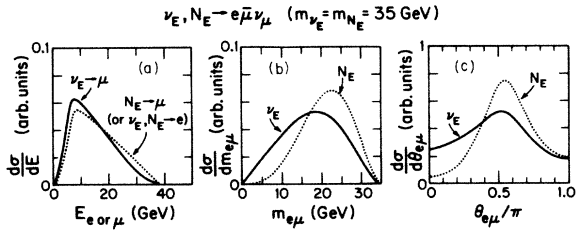

FIG. 2. Distributions from ν_E, N_E decays to $e\bar{\mu}\nu_\mu$ with the ν_E, N_E pair produced in e^+e^- collisions on the Z resonance, taking $m_{\nu_E} = m_{N_E} = 35$ GeV. (a) Electron or muon energy; (b) $e\bar{\mu}$ invariant mass; (c) angular separation of $e\bar{\mu}$.

$Z \to E^+E^-, \nu_E\bar{\nu}_E, N_E\bar{N}_E$ channels will yield copious events to study, but for the present the best opportunities arise from the decays of W bosons produced at $p\bar{p}$ colliders: $W \to E\nu_E, EN_E$.

The experimental signature for exotic W decays depends critically on the lepton mass ordering. We shall assume that all three exotic leptons are heavy (tens of GeV) and distinguish the two principal scenarios A and B of Sec. II according to whether E is heavier or lighter than ν_E, N_E.

Exotic quarks can be produced directly in $p\bar{p}$ collisions via the QCD quark and gluon fusion subprocesses $q\bar{q} \to h\bar{h}, gg \to h\bar{h}$.

A. Scenario A: $m_E > m_{\nu_E}, m_{N_E}$

In this case, assuming minimal intergenerational mixing, we expect the E and $\nu_E(N_E)$ decays to proceed mainly by charged-current transitions,

$$E \to \nu_E(N_E) + (\text{virtual } W \to q\bar{q}, l\bar{\nu}) ,$$
$$\nu_E(N_E) \to e + (\text{virtual } W \to q\bar{q}, \nu\bar{l}) , \tag{21}$$

where e denotes the light conventional charged lepton belonging to the same generation as E. Hence we obtain typically

$$W \to E\bar{\nu}_E(\bar{N}_E) \to e\bar{e}qqq\bar{q}\,\bar{q}\,\bar{q} , \tag{22}$$

for which the signature is one or two identified electrons plus jets with invariant mass $\approx m_W$ and no significant missing p_T. Leptonic modes of the virtual W decays in Eq. (21) can give additional leptons and missing p_T, however.

B. Scenario B: $m_E < m_{\nu_E}, m_{N_E}$

In this case, with similar reasoning, we expect the E and $\nu_E(N_E)$ decays to proceed mainly by the transitions

$$\nu_E(N_E) \to E + (\text{virtual } W \to q\bar{q}, \nu\bar{l}) ,$$
$$E \to \nu + (\text{virtual } W \to q\bar{q}, l\bar{\nu}) , \tag{23}$$

where ν denotes the light conventional neutrino of the same generation. For these decays we obtain typically

$$W \to E\bar{\nu}_E(\bar{N}_E) \to \nu\bar{\nu}qqq\bar{q}\,\bar{q}\,\bar{q} \tag{24}$$

for which the signature is missing p_T plus jets. The decays $E \to e + (\text{virtual } Z)$ and $\nu_E \to E + (\text{virtual } W)$ give the signature in Eq. (22) at a smaller rate than in scenario A.

C. Other scenarios

If the mass ordering were split, e.g., $m_{N_E} > m_E > m_{\nu_E}$, various things could happen: (i) $W \to E\bar{N}_E$ could be kinematically disallowed, leaving scenario A for the remaining mode; (ii) $W \to E\bar{N}_E$ could be allowed, with $\bar{N}_E \to \bar{E} \to \bar{\nu}_E$ cascade decay, again leaving approximately scenario A.

If E, ν_E, N_E were closely degenerate, the $E \leftrightarrow \nu_E(N_E)$ decays could be suppressed and both heavy leptons might decay directly to light leptons giving $W \to e\bar{\nu}q\bar{q}\,\bar{q}$ typically. This has a different signature, lepton plus missing p_T plus jets, somewhat like the top signal $W \to t\bar{b} \to e\nu b\bar{b}$; we shall not pursue it here.

Below we present illustrative calculations of the signals for scenarios A and B in $p\bar{p}$ collisions at $\sqrt{s} = 630$ GeV.

D. Illustrative calculations

We set out to compare predicted exotic E_6 signals with three types of data collected at the CERN $p\bar{p}$ collider by the UA1 Collaboration predominantly at the c.m. energy $\sqrt{s} = 630$ GeV.

(i) Single isolated electron plus jets:[20] this relates to first-generation leptons in scenario A or B and any-generation h.

(ii) Dimuons, both isolated and nonisolated:[21] this relates to second-generation leptons in scenario A or B and any-generation h.

(iii) Large missing p_T (denoted $\not{p}_T$):[22] this relates to any generation of leptons in scenario B.

We calculate W production in $p\bar{p}$ collisions using the truncated shower model of Ref. 23. This is based on the parton subprocess $u\bar{d} \to W^+g$ which correctly describes the large-p_T behavior of W production and the dominant 0-jet and 1-jet channels; an empirical cutoff on the small-p_T divergence reproduces the correct total cross section. We use the Duke-Owens model 1 parton distributions[24] with $\Lambda = 0.2$ GeV and $Q^2 = \hat{s}$ the subprocess c.m. energy squared.

The squared matrix element for the overall production and decay process $u\bar{d} \to e\bar{e}\,qqq\,\bar{q}\,\bar{q}\,\bar{q}g$, including all spin correlations, can be derived compactly for the case of $V-A$ couplings.[25] (The case of two final neutrinos is similar.) For simplicity, we take the same matrix element also for the mixed $V \pm A$ cases involving N_E; the dominant consideration is phase space, which is treated exactly throughout. The final-state gluon and quarks are coalesced into jets, using the algorithm by which the UA1 Collaboration combines calorimeter cells into jets.[20–22] The possible appearance of lepton pairs $l\bar{\nu}$ in place of some of the $q\bar{q}$ pairs is a secondary complication, ignored in this initial treatment. We normalize at $\sqrt{s} = 630$ GeV to the observed W-production cross section of 6 nb and assume branching fractions for each generation[11]

TABLE IV. Isolated single electron plus jets from $W \to E\nu_E, EN_E$: cross sections in pb.

Masses (GeV)		$\sigma(e+n$ jets) vs n						
E	ν_E, N_E	0	1	2	3	4	5	Total
40	35		2	22	44	22	3	93
45	25		2	19	35	19	3	78
30	25		18	69	79	29	2	197
45	5			4	4			8

$$B(W \to E\nu_E) = B(W \to EN_E) = 0.07 f \ , \tag{25}$$

$$f = [1-2(x_1+x_2)+(x_1-x_2)^2]^{1/2} \times [1-\tfrac{1}{2}(x_1+x_2)-\tfrac{1}{2}(x_1-x_2)^2] \ , \tag{26}$$

where f is the normal mass-dependence factor and $x_1 = m_E^2/m_W^2, x_2 = m_{\nu_E}^2/m_W^2$, with approximate degeneracy $m_{\nu_E} \approx m_{N_E}$.

We calculate $h\bar{h}$ production using the lowest-order QCD subprocesses (with no K factor) folded with the Duke-Owens parton distributions above for a range of h masses. We assume h fragments into an h hadron of essentially the same mass and momentum, and approximate the subsequent charged-current (CC) and neutral-current (NC) decays into electrons or muons by the bare-quark matrix elements.

E. $W \to E\nu_E$ (EN_E) signals in scenario A

For the single-electron signal we take the acceptance cuts of the UA1 top-quark search, namely,[20]

$$p_T(e) > 12 \text{ GeV}, \quad |\eta(e)| < 3 \ , \tag{27}$$

$$p_T(\text{jet } 1) > 8 \text{ GeV}, \quad p_T(\text{jet } n \geq 2) > 7 \text{ GeV} \ , \quad |\eta(\text{jet})| < 2.5 \ , \tag{28}$$

with electron-isolation criteria

$$\sum E_T(\Delta R < 0.4) < 1 \text{ GeV} \ , \quad \sum E_T(\Delta R < 0.7) < 2 \text{ GeV} \ . \tag{29}$$

Here the summations are over hadronic E_T within cones about the electron direction, defined in terms of ΔR, where

$$(\Delta R)^2 = (\Delta\eta)^2 + (\Delta\phi)^2 \ . \tag{30}$$

In this case the second (unidentified) electron is added into the jets. The calculated single-lepton signal is substantial; Table IV gives some examples. The biggest cross sections occur when both masses are of order 20–30 GeV; when ν_E gets much lighter, the isolation cuts get more severe; when the sum of masses approach m_W, the factor f gets small.

Taking integrated luminosity 0.39 pb^{-1} corresponding to runs that have been analyzed and detection efficiency of order 50%, this scenario with favorable mass values would predict 15–35 e plus $n \geq 2$-jet events satisfying the UA1 cuts, of which 10–20 events have $n \geq 3$ jets. Recent preliminary results from the UA1 top-quark search[20] in these same $e+n$-jet configurations indicate a total of about 13 events with $n \geq 2$ of which only 4 events have $n \geq 3$ jets. From these preliminary data it appears that scenario A with "favorable" mass values (such as the first three entries in Table IV) can already be excluded for exotic leptons of the first generation.

Figure 3 illustrates the $p_T(e)$ spectrum and the invariant mass of e plus jets for the case on the top line of Table IV.

There is also a possible e^+e^- or $\mu^+\mu^-$ dilepton signal in this scenario. To discuss this we adopt the latest acceptance cuts of the UA1 dimuon analysis[21]

$$p_T(\mu) > 3 \text{ GeV}, \quad |\eta(\mu)| < 2.0 \ , \quad m(\mu\bar{\mu}) > 6 \text{ GeV} \ . \tag{31}$$

Dimuons are classified as "isolated" or "nonisolated" depending on the amount of hadronic E_T contained in a cone $\Delta R < 0.7$ about each muon. An event is classified as isolated, in the latest discussion, if

$$\left[\sum E_T\right]_{\mu_1}^2 + \left[\sum E_T\right]_{\mu_2}^2 < (3 \text{ GeV})^2 \ . \tag{32}$$

Our calculations contain an estimate of E_T contributions from the underlying event. Examples of our results are shown in Table V.

With integrated luminosity of 0.39 pb^{-1} and efficiency factors 0.45×0.58 from chamber geometry and track quality, these results predict 10–20 unlike-sign dimuons—equally divided between isolated and nonisolat-

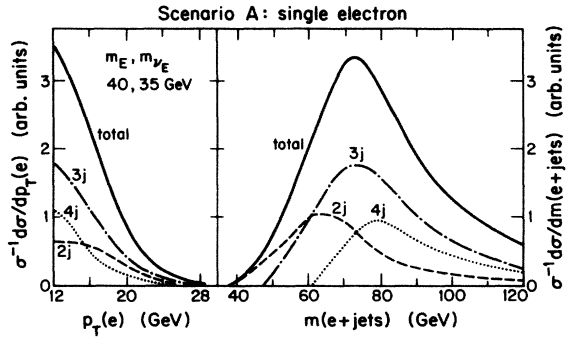

FIG. 3. Isolated-single-electron signal from $W \to E\nu_E, EN_E$ (scenario A) dependence on $p_T(e)$ and invariant mass $m(e+\text{jets})$ for UA1 cuts. Solid curves denote the total signal; the dominant two-, three-, and four-jet contributions are shown as dashed, dot-dashed, and dotted curves, respectively. The case illustrated is that on the top line of Table IV.

TABLE V. Dimuon cross sections from $W \to E\nu_E, EN_E$ for isolated (I) and nonisolated (NI) events, with normal UA1 mass cut $m > 6$ GeV and high-mass cut $m > 20$ GeV.

Masses (GeV)		σ (pb)			
E	ν_E, N_E	I ($m>6$)	I ($m>20$)	NI ($m>6$)	NI ($m>20$)
40	35	43	14	56	22
45	25	41	12	68	20
30	25	78	35	107	56

ed categories for the standard mass cut above. These numbers are small compared with preliminary UA1 results with this luminosity and efficiency, to wit 150 $\mu^+\mu^-$ events, 44 isolated (I), 106 nonisolated (NI). The UA1 results are already quite well explained by conventional Drell-Yan plus Υ plus heavy-quark sources,[23] but some small exotic contributions are not necessarily excluded. To tighten the analysis we impose the more stringent mass cut $m(\mu\mu) > 20$ GeV; in this range the exotic-lepton source predicts 3—9 events, whereas the data include only 4 events (2 I, 2 NI) which are already well accounted for by conventional mechanisms. We also note that most of the E_6-exotic dimuons have muon-plus-jets invariant mass of order m_W, unlike most Drell-Yan or Υ or $b\bar{b}$-generated dimuon events.

It appears that present dimuon data already cast doubt on more favorable mass assignments, such as those in Table V for exotic leptons of the second generation in this scenario. When the values of μ+jets invariant mass are made public, it may be possible to tighten the constraints further. Figure 4 shows the $p_T(\mu\mu)$ and $m(\mu\mu)$ distributions for the first and third examples in Table V.

F. $W \to E\nu_E, EN_E$ signals: Scenario B

Here we are concerned first with a missing-p_T ($\not{p}_T$) signal. Conventional physics sources[26] can contribute large backgrounds for $\not{p}_T < 20$ GeV, and it appears that these backgrounds only become small for $\not{p}_T > 40$ GeV, at the CERN $p\bar{p}$ collider. Our calculations assume that E decays 77% by charged current to light neutrinos, and refer to the contribution of a single generation; for the case of three degenerate generations of exotic leptons, multiply the results by three.

Table VI illustrates the predicted cross sections for $\not{p}_T > 20$, 30, and 40 GeV, with several mass assignments. For typical luminosity 0.39 pb^{-1} and efficiency of order 50%, these results indicate at best about 1 event with $\not{p}_T > 30$ and only 0.1 event in the relatively clean region $\not{p}_T > 40$ GeV. In the latter region the UA1 Collaboration has a few events which may not have conventional explanations. It appears that the present experimental data on large $\not{p}_T$ cannot place significant bounds on exotic leptons in this scenario even if three generations contribute.

Figure 5 shows the $\not{p}_T$ dependence of the signal, for the example in the top line of Table VI. Clearly this mechanism gives relatively small values of $\not{p}_T$. In the region $\not{p}_T > 40$ GeV, about 80% of the events have 2 or 3 jets.

The single-electron signal from this scenario is about one-third that of scenario A, for corresponding values of masses (i.e., in Table IV interchange the first two columns and divide the entries in the other columns by 3). This is potentially a much more restrictive test of scenario B. Present data appear to exclude only the region near $m_{\nu_E} = 30$ GeV, $m_E = 25$ GeV, which are somewhat more restrictive than the e^+e^- limits.

The dimuon signal is only about one-tenth of that from scenario A and therefore leads to no significant constraints.

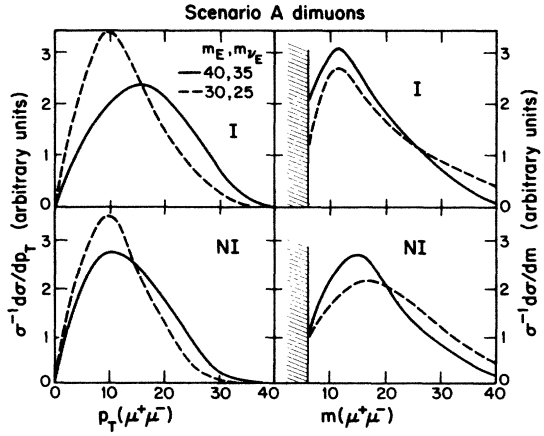

FIG. 4. Dimuon signal from $W \to E\nu_E$, EN_E (scenario A) dependence on $p_T(\mu\mu)$ and $m(\mu\mu)$ for isolated (I) and nonisolated (NI) events, with UA1 cuts. Solid curves denote the case in the top line of Table V, dashed curves denote the case in the bottom line.

G. $h\bar{h}$ signals

We calculate below the signal from $h\bar{h}$ belonging to a single generation. If the h quarks from all three generations are degenerate, these results must be multiplied by three.

When either h or $\bar{h}$ decays semileptonically by charged currents, a single-lepton signal arises. We impose the

TABLE VI. Missing p_T from $W \to E\nu_E, EN_E$, scenario B.

Masses (GeV)		σ (pb)		
E	ν_E, N_E	$\not{p}_T > 20$ GeV	$\not{p}_T > 30$ GeV	$\not{p}_T > 40$ GeV
35	40	31	2	0.2
25	45	17	1	0.1
25	30	34	3	0.3

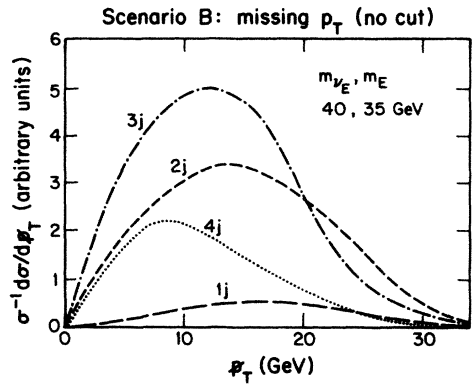

FIG. 5. Missing-p_T signal from $W\to E\nu_E, EN_E$ (scenario B) for the case on the top line of Table VI. The one-, two-, three-, and four-jet contributions are denoted by long-dashed, short-dashed, dash-dotted, and dotted curves, respectively.

same cuts as in Sec. IV E for isolated electron plus jets. Table VII illustrates the predicted cross sections for a range of h masses, assuming semileptonic branching fraction 8% as in Sec. II. With an integrated luminosity 0.39 pb^{-1} and efficiency 50%, these figures indicate of order 13–30 events with $n\geq 2$ jets, of which 6–8 have $n\geq 3$. These exceed or at least saturate the corresponding UA1 data containing 13 events with $n\geq 2$, 4 events with $n\geq 3$. It appears that these data are not compatible with a single h quark having mass ≤ 30 GeV.

The limit above depends on the integrated jet cross sections alone, and could probably be made more stringent by examining other properties of the predicted events. Figure 6 shows the dependence on $p_T(e)$ and on the invariant mass $m(e+\text{jets})$ for the case of $m_h=30$ GeV.

There are also dilepton signals from $h\bar{h}$ decays, arising from both charged-current (CC) and neutral-current (NC) mechanisms. The former occur when both h and $\bar{h}$ have semileptonic CC decays $h\to ul\bar{\nu}, \bar{h}\to\bar{u}\nu\bar{l}$ (we assume 8% branching fraction for each channel $l=e,\mu,\tau$); these give

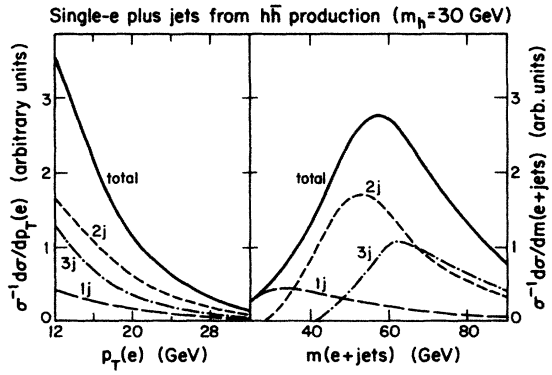

FIG. 6. Isolated-electron signal from $h\bar{h}$ production at $\sqrt{s}=630$ GeV and with UA1 cuts for the case $m_h=30$ GeV. Solid curves denote the total signal; the dominant one-, two-, and three-jet contributions are denoted by long-dashed, short-dashed, and dash-dotted curves, respectively.

TABLE VII. Single e plus jets from $h\bar{h}$. Cross sections in pb.

h mass (GeV)	$\sigma(e+n$ jets) vs n 0	1	2	3	4	Total
25	4	60	110	40	1	215
30	1	18	60	38	3	120
35		5	31	29	4	70

e^+e^-, μ^+e^-, $e^+\mu^-$, and $\mu^+\mu^-$ plus hadrons. We have calculated the $\mu^+\mu^-$ signals at $\sqrt{s}=630$ GeV with the cuts previously described, corresponding to the UA1 dimuon measurements. The resulting cross sections are shown in Fig. 7 and listed in Table VIII.

The NC dileptons come from $h\to d\bar{l}\bar{l}$ decay or the corresponding $\bar{h}$ decay (we assume 1% branching fraction for each lepton flavor), which give e^+e^- and $\mu^+\mu^-$ signals. Again we calculate the dimuon case with UA1 cuts; the resulting cross sections are shown in Table IX. Since both muons come from the same parent, $m(\mu\mu)<m_h$ for these signals; the fraction of events with $m(\mu\mu)>20$ GeV increases with m_h, but the total signal decreases because the basic $h\bar{h}$ production cross section falls steeply.

The total CC + NC dimuon signal from $h\bar{h}$ production is appreciably smaller than the exotic-lepton examples previously shown in Table V. For integrated luminosity 0.39 pb^{-1} and efficiency factors 0.45×0.58 as before, the total predicted $h\bar{h}$ events are at most 6 isolated and 2 non-isolated dimuons compared with 44 isolated and 106 non-isolated $\mu^+\mu^-$ reported by the UA1 collaboration. It will not be easy to place bounds on this possible contribution, but clearly isolated dimuons are the most promising set to study; those of $h\bar{h}$ origin may be expected to have typically much more accompanying hadronic E_T than Drell-Yan and Υ events, but may be more difficult to discriminate from $b\bar{b}$ events. Figure 7 shows the predicted dependence

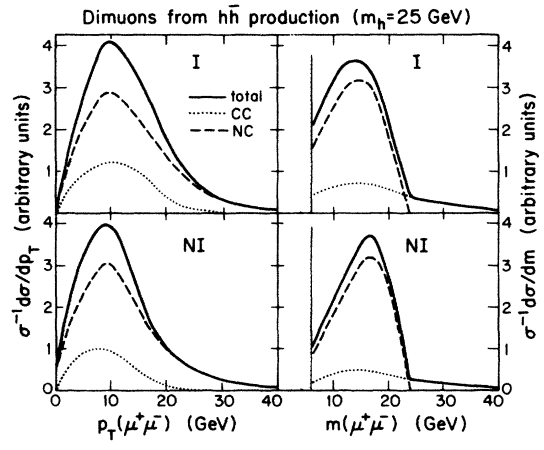

FIG. 7. Dimuon signals from $h\bar{h}$ production at $\sqrt{s}=630$ GeV with UA1 cuts for isolated (I) and nonisolated (NI) events, with $m_h=25$ GeV. Solid curves denote the total signal; the CC and NC contributions are denoted by dotted and dashed curves, respectively.

TABLE VIII. CC dimuons from $h\bar{h}$ at $\sqrt{s}=630$ GeV; cross sections in pb for isolated (I) and nonisolated (NI) events, with normal UA1 mass cut $m>6$ GeV and high-mass cut $m>20$ GeV.

h mass	σ (pb)			
(GeV)	I ($m>6$)	I ($m>20$)	NI ($m>6$)	NI ($m>20$)
25	15	6	5	2
30	7	2	3	1
35	3	1	2	0.6

of $h\bar{h}$ dimuon events on $p_T(\mu\mu)$ and $m(\mu\mu)$ for the case $m_h=25$; as one might expect from their different origins, the high-p_T tail is due to NC events, whereas the high-m tail is due to CC contributions.

H. Summary of restrictions from $p\bar{p}$ data

The restrictions found above from the CERN $p\bar{p}$ collider data may be summarized as follows.

(i) $W\to E\nu_E(EN_E)$ with scenario A ($m_E>m_{\nu_E},m_{N_E}$). Isolated electron-plus-jet data[20] conflict with this scenario for the first generation if the mass assignments are favorable, as, for example, in the first three lines of Table IV. Dimuon data also cast doubt on these cases for the second generation.

(ii) $W\to E\nu_E(EN_E)$ with scenario B ($m_E<m_{\nu_E},m_{N_E}$). Missing-p_T data[22] impose no real restrictions here. Isolated electron data provide limited restrictions.

(iii) $h\bar{h}$ hadroproduction. Isolated-electron data[20] exclude values of $m_h\lesssim 30$ GeV for any generation. Present dimuon data are not yet detailed enough to place constraints.

I. Very heavy exotics

If the h quark is heavier than the Z boson, but lighter than $\frac{1}{2}M_{Z'}$, then it can be produced in the decay $Z'\to h\bar{h}$ with branching fraction[11] up to 20%, depending on the number of exotic states accessible in Z' decays and the extent of phase-space suppression. For still higher h mass, it can be produced in hadron collisions via the QCD subprocesses $q\bar{q},gg\to h\bar{h}$. Figure 8 shows the expected $p\bar{p}$ and pp cross sections for various h-mass values versus $\sqrt{s}$ up to the highest energies anticipated at supercolliders; $p\bar{p}$ and pp results are similar well above $h\bar{h}$ thresholds. Single h production via $Wu\to h$ and $gu\to Wh$ and similar subprocesses $Zd\to h,gd\to Zh$ may also be significant at the highest supercollider energies.[27]

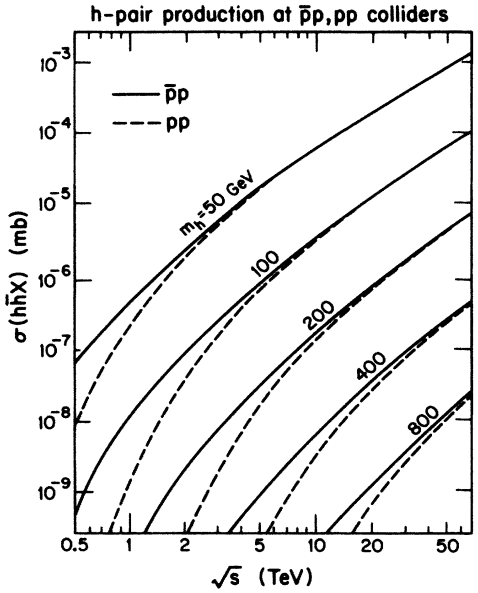

FIG. 8. Energy dependence of $h\bar{h}$ production by lowest-order QCD fusion mechanisms, for $m_h=50$, 100, 200, 400, 800 GeV. Solid lines denote production by $p\bar{p}$; dashed lines denote production by pp collisions.

Very massive h quarks decay to real W and Z bosons. (See, for example, Ref. 28.) The partial widths for these decays are

$$\Gamma(h\to uW)=\sin^2\alpha_h\frac{G_F m_h{}^3}{8\sqrt{2}\pi}(1+2M_W{}^2/m_h{}^2)(1-M_W{}^2/m_h{}^2)^2\,,$$
$$\Gamma(h\to dZ)=\sin^2\alpha_h\cos^2\alpha_h\frac{G_F m_h{}^3}{16\sqrt{2}\pi}(1+2M_Z{}^2/m_h{}^2)(1-M_Z{}^2/m_h{}^2)^2\,, \tag{33}$$
$$\Gamma(h\to dZ')=\sin^2\alpha_h\cos^2\alpha_h\frac{G_F m_h{}^3}{4\sqrt{2}\pi}(1+2M_{Z'}{}^2/m_h{}^2)(1-M_{Z'}{}^2/m_h{}^2)^2\,.$$

If m_h is much larger than any of these gauge-boson masses, the relative widths are

$$\Gamma(h\to uW):\Gamma(h\to dZ):\Gamma(h\to dZ')\approx 2:1:4\,. \tag{34}$$

Very massive leptons pair-produced via virtual γ, Z, or Z' would likewise decay to W,Z bosons. In scenario A the exotic leptons would decay dominantly by charged currents, $E\to\nu_E W,N_E W$ and $\nu_E,N_E\to eW$. In scenario B the ν_E,N_E would decay by charged currents $\nu_E,N_E\to EW$ while the charged E lepton would decay both by charged

TABLE IX. NC dimuons from $h\bar{h}$ at $\sqrt{s}=630$ GeV; cross sections in pb for isolated (I) and nonisolated (NI) events, with normal UA1 mass cut $m>6$ GeV and high-mass cut $m>20$ GeV.

h mass	σ (pb)			
(GeV)	I ($m>6$)	I ($m>20$)	NI ($m>6$)	NI ($m>20$)
25	42	4	18	2
30	19	5	8	3
35	9	4	4	2

and neutral currents in the proportions

$$\Gamma(E\to\nu_e W):\Gamma(E\to eZ):\Gamma(E\to eZ') = 2\sin^2(\alpha_E-\alpha_\nu):\sin^2\beta_E\cos^2\beta_E:4\sin^2\beta_E\cos^2\beta_E\ . \tag{35}$$

V. LIMITS ON FCNC

Because the I_{3L} and $\tilde{Q}$ quantum numbers of exotic fermions are different than those of the known fermions, mixing for left- and right-handed states is not the same. The FCNC contributions in Fig. 9 associated with Z and Z' arise from mixings of left-handed charge $-\frac{1}{3}$ quarks and right-handed charged leptons. (There is a Glashow-Iliopoulos-Maiani cancellation in the right-handed quark sector and in the left-handed lepton sectors.) We present our results in terms of individual FCNC coupling strengths rather than model-dependent mixing angles.

A. $K_L, K_S\to\bar{\mu}\mu$

The relevant part of the Lagrangian is

$$\mathscr{L} = \frac{G_F}{\sqrt{2}}[\bar{d}\gamma^\mu(1-\gamma_5)sA_{ds}+\text{H.c.}] \times\bar{\mu}\gamma^\mu[(-\tfrac{1}{2}+\tfrac{1}{3}\eta^2)(1-\gamma_5)+\tfrac{2}{3}\eta^2(1+\gamma_5)+2x_W]\mu\ , \tag{36}$$

where A_{ds} denotes the strength of induced sd FCNC, and higher-order mixing terms in the muon current are ignored. The matrix element for $K_{S,L}$ decay to $\bar{\mu}\mu$ is

$$\mathscr{M} = \frac{G_F}{\sqrt{2}}f_K\frac{A_{ds}\pm A_{ds}^*}{\sqrt{2}}m_\mu(1+\tfrac{2}{3}\eta^2)\bar{\mu}\gamma_5\mu \tag{37}$$

and

$$\Gamma(K_{S,L}\to\bar{\mu}\mu) = \frac{G_F^2 f_K^2 m_\mu^2 m_K}{16\pi}(1+\tfrac{2}{3}\eta^2)^2\left|\frac{A_{ds}\pm A_{ds}^*}{\sqrt{2}}\right|^2 \times\left[1-\frac{4m_\mu^2}{m_K^2}\right]^{1/2} \tag{38}$$

The measured values $\Gamma(K_S\to\bar{\mu}\mu)/\Gamma(K_S\to\text{all})<3.2\times10^{-7}$ and $\Gamma(K_L\to\bar{\mu}\mu)/\Gamma(K_L\to\text{all})=(9\pm2)\times10^{-9}$ give the constraints (for $\eta=0$)

$$|\,\text{Re}(A_{ds})\,|<3\times10^{-3}\ , \tag{39a}$$

$$|\,\text{Im}(A_{ds})\,|<2\times10^{-5}\ . \tag{39b}$$

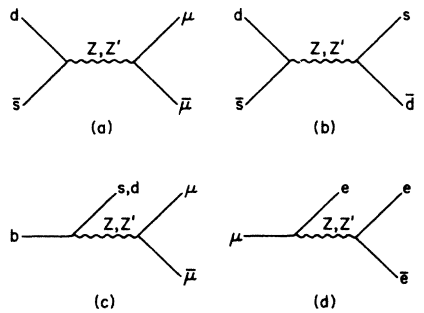

FIG. 9. Flavor-changing neutral-current contributions due to Z,Z' in the processes (a) $K_{L,S}\to\mu\bar{\mu}$, (b) K_L,K_S mixing, (c) $b\to q\mu\bar{\mu}$, and (d) $\mu\to e\bar{e}e$.

B. K_L-K_S mass difference

The effective Lagrangian is

$$\mathscr{L}_{\text{eff}}^{\Delta S=2} = \frac{G_F}{4\sqrt{2}}(1+4\eta^2)[\bar{d}\gamma^\mu(1-\gamma_5)sA_{ds}]^2\ , \tag{40}$$

which leads to the matrix element

$$\langle\bar{K}^0|\,\mathscr{L}_{\text{eff}}^{\Delta S=2}\,|K^0\rangle = \frac{G_F}{4\sqrt{2}}f_K^2 B m_K^2\tfrac{8}{3}(1+4\eta^2)A_{ds}^2\ , \tag{41}$$

where bag factor B (of order 0.3–1) is the deviation from the vacuum saturation calculation. Then

$$\frac{\Delta m_K}{m_K} = \frac{\text{Re}\langle\bar{K}^0|\,\mathscr{L}_{\text{eff}}^{\Delta s=2}\,|K^0\rangle}{m_K^2} = \frac{2}{3}\frac{G_F}{\sqrt{2}}f_K^2 B(1+4\eta^2)\text{Re}(A_{ds}^2)\ , \tag{42}$$

where combined with Eq. (39b) the experimental value $\Delta m_K/m_K=7\times10^{-15}$ gives

$$[\text{Re}(A_{ds}^2)]^{1/2}<3.6\times10^{-4}/B^{1/2}\ . \tag{43}$$

C. $b\to q\bar{\mu}\mu$ ($q=d$ or s)

The effective Lagrangian is

$$\mathscr{L}_{\text{eff}} = \frac{8G_F}{2}\tfrac{1}{4}A_{qb}\bar{q}\gamma^\mu(1-\gamma_5) \times b\bar{\mu}\gamma^\mu[-\tfrac{1}{4}+x_W+\tfrac{1}{2}\eta^2+(\tfrac{1}{4}+\tfrac{1}{6}\eta^2)\gamma_5]\mu\ , \tag{44}$$

where A_{qb} is the strength of the bq FCNC for $q=d$ or s. The resulting decay rate is

$$\Gamma(b\to q\bar{\mu}\mu) = \frac{G_F^2 m_b^5}{192\pi^3}\frac{(1-4x_W-2\eta^2)^2+(1+\frac{2}{3}\eta^2)^2}{8}\,|\,A_{sb}\,|^2 \tag{45}$$

and hence

$$\frac{\Gamma(b\to q\bar{\mu}\mu)}{\Gamma(b\to c\mu\bar{\nu})} = \frac{(1-4x_W-2\eta^2)^2+(1+\frac{2}{3}\eta^2)^2}{8}\frac{|\,A_{sb}\,|^2}{|\,U_{cb}^{\text{KM}}\,|^2\rho}\ , \tag{46}$$

where U_{cb}^{KM} is the usual Kobayashi-Maskawa mixing matrix element and ρ (≈0.43) is a phase-space suppression factor for $b\to c$ decays. Imposing the experimental limit $\Gamma(b\to\bar{\mu}\mu X)/\Gamma(b\to\mu\bar{\nu}X)<0.003/0.13$ and assuming that the $b\to c$ transition is not significantly modified by quark mixing with exotics, we find the limit

$$|\,A_{qb}\,|<0.28\,|\,U_{cb}^{\text{KM}}\,|\ ,\quad q=d\text{ or }s\ . \tag{47}$$

D. $\mu \to e\bar{e}e$, $\tau \to \mu\bar{\mu}\mu$, $\tau \to e\bar{e}e$

The effective Lagrangian for $\mu \to e\bar{e}e$ is

$$\mathcal{L}_{\text{eff}} = \frac{8G_F}{\sqrt{2}}(-\tfrac{1}{4})\bar{e}\gamma^\mu(1+\gamma_5)\mu B_{e\mu}\bar{e}\gamma^\mu[-\tfrac{1}{4}+x_W+\tfrac{1}{2}\eta^2+(\tfrac{1}{4}+\tfrac{1}{6}\eta^2)\gamma_5]e \ , \tag{48}$$

where $B_{e\mu}$ is the strength of the e-μ FCNC.

The presence of identical particles in the final states leads to a decay rate which differs in form from the three-body $b \to q\bar{\mu}\mu$ decay rate above. We find

$$\Gamma(\mu \to e\bar{e}e) = \frac{G_F^2 m_\mu^5}{192\pi^3}\frac{|B_{e\mu}|^2}{16}[3(1-2\eta^2)^2+3(1-4x_W-2\eta^2)^2+2(-1+4x_W+2\eta^2)(1-2\eta^2)] \ . \tag{49}$$

Similar formulas hold for $\tau \to \mu\bar{\mu}\mu$ and $\tau \to e\bar{e}e$ with $B_{e\mu}$ replaced by $B_{\mu\tau}$ and $B_{e\tau}$, respectively. From the experimental bounds $B(\mu \to e\bar{e}e) < 1.9\times10^{-9}$, $B(\tau \to \mu\bar{\mu}\mu) < 4.9\times10^{-4}$, and $B(\tau \to e\bar{e}e) < 4.0\times10^{-4}$ and the observed branching ratios $B(\tau \to \mu\nu\bar{\nu}) = 0.185$, $B(\tau \to e\nu\bar{\nu}) = 0.165$, we deduce

$$|B_{e\mu}| < 1\times10^{-4}, \quad |B_{\mu\tau}| < 0.12 \quad |B_{e\tau}| < 0.11 \ . \tag{50}$$

Slightly larger limits are found from the experimental bounds on $\tau \to \mu\bar{e}e$ and $\tau \to e\bar{\mu}\mu$. Once again we have to assume the approximate universality of charge currents.

The η^2 terms in the above FCNC effects were from Z' contributions in the effective interaction. This increases the predicted rates by as much as 40% for the allowed values of η. The limits we quoted above, for $\eta = 0$, are therefore more conservative than the general two-Z result.

VI. WEAK-UNIVERSALITY CONSTRAINTS

The observed universality of weak-charged-current interactions also places constraints on fermion mixings.[29] We consider only the effects of mixing in the neutral-lepton sector between known and heavy ($\gtrsim 1$ GeV) exotics; mixing is known to be small for the light neutral exotics, as discussed in Sec. III. We define A_l to be the strength of the charge-current coupling of a known charged lepton l and its neutrino ν_l; deviations of A_l from unity imply a violation of weak universality.

A. $^{14}O \to {}^{14}N\, e\bar{\nu}_e$ vs $\mu \to \nu_\mu e\bar{\nu}_e$ decays

The experimental constraint from the ratio of these decay rates is

$$|U_{ud}^{\text{KM}}| / \sqrt{A_\mu} = 0.9737 \pm 0.0025 \ . \tag{51}$$

The mixing in the electron sector drops out of the ratio of decay rates.

B. $\pi \to e\bar{\nu}_e$ vs $\pi \to \mu\bar{\nu}_\mu$ decays

Comparison of the experimental measurements and the theoretical decay rates, including radiative corrections, yields the constraint

$$A_e / A_\mu = 0.9878 \pm 0.0114 \ . \tag{52}$$

C. τ decays

The τ leptonic branching fractions are related to the τ and μ decay widths by

$$B(\tau \to e\nu_\tau\bar{\nu}_e) = \frac{A_\tau}{A_\mu}\left[\frac{m_\tau}{m_\mu}\right]^5\frac{\Gamma_\mu}{\Gamma_\tau} \ ,$$
$$B(\tau \to \mu\nu_\tau\bar{\nu}_\mu) = 0.973\frac{A_\tau}{A_e}\left[\frac{m_\tau}{m_\mu}\right]^5\frac{\Gamma_\mu}{\Gamma_\tau} \ , \tag{53}$$

where 0.973 is a phase-space factor. From the current experimental values we find

$$A_\tau / A_\mu = 0.927 \pm 0.124 \ ,$$
$$A_\tau / A_e = 1.014 \pm 0.127 \ . \tag{54}$$

If all mixings between the known and exotic left-handed leptons are negligibly small, then $A_e \simeq A_\mu \simeq A_\tau \simeq 1$ and Eq. (51) measures U_{ud}^{KM}. On the other hand, if the mixings between known and exotic left-handed quarks are negligible, then unitarity of U^{KM} combined with measurements of U_{ud}^{KM}, U_{us}^{KM}, and U_{ub}^{KM} give[29]

$$|U_{ud}^{\text{KM}}| > 0.9748 \tag{55}$$

and hence

$$\sqrt{A_\mu} \geq 0.996, \quad \sqrt{A_e} \geq 0.978, \quad \sqrt{A_\tau} \geq 0.853 \ , \tag{56}$$

at the 2σ level.

VII. SUMMARY

We have studied the observable consequences of the presence of exotic fermions belonging to E_6 **27** representations, which are suggested by some superstring models. We have concentrated on mixing of exotics only within the same generation. We find the following.

(i) The exotic h quark has semileptonic neutral-current decays at the few percent level; fully reconstructable final states like $d\bar{l}\bar{l}$ could be used to determine its mass.

(ii) There are two principal scenarios for exotic leptons, depending on whether m_E is (A) greater than or (B) less than m_{ν_E}, m_{N_E}. In (A) charged-current modes dominate the decays of E, ν_E, and N_E whereas in (B) the E lepton has appreciable neutral-current decays.

(iii) In e^+e^- collisions, Z-boson decays would be a copious source of E, ν_E, and N_E exotic leptons if kinematically allowed; the h quark and N,n leptons could be copiously produced in Z' decays.[11]

(iv) In $p\bar{p}$ collisions, W decays to exotic leptons, and hadronic $h\bar{h}$ production are potential sources.

(v) Isolated electron data at the CERN collider already place significant bounds on exotic first-generation lepton masses in scenario A. Dimuon data constrain second-generation lepton masses in this scenario. For example, in each case the top three lines of Tables IV and V are excluded.

(vi) Collider data do not greatly restrict exotic-lepton scenario B, however.

(vii) Isolated-electron data exclude exotic-h-quark masses $\lesssim 30$ GeV for any generation.

(viii) Very heavy exotics will decay to real W and Z bosons.

(ix) Most of our results are not dependent on the existence of a light Z' boson.

ACKNOWLEDGMENTS

This research was supported in part by the University of Wisconsin Research Committee with funds granted by the Wisconsin Alumni Research Foundation, and in part by the U.S. Department of Energy under Contracts Nos. DE-AC02-76ER00881 and DE-FG06-85ER40224.

[1]E. Witten, Phys. Lett. **155B**, 151 (1985); Nucl. Phys. **B258**, 75 (1985).

[2]P. Candelas, G. T. Horowitz, A. Strominger, and E. Witten, Nucl. Phys. **B258**, 46 (1985).

[3]J. D. Breit, B. A. Ovrut, and G. Segré, Phys. Lett. **158B**, 33 (1985).

[4]A. Sen, Phys. Rev. Lett. **55**, 33 (1985).

[5]P. Binétruy, S. Dawson, I. Hinchliffe, and M. Sher, Lawrence Berkeley Laboratory Report No. 203173, 1985 (unpublished).

[6]J. Rosner, Enrico Fermi Institute Report No. EFI 85-34, 1985 (unpublished).

[7]E. Cohen, J. Ellis, K. Enquist, and D. V. Nanopoulos, Phys. Lett. **165B**, 76 (1985).

[8]R. Robinett, University of Massachusetts Report No. UMHEP-239, 1985 (unpublished).

[9]S. M. Barr, Phys. Rev. Lett. **55**, 2778 (1985).

[10]L. S. Durkin and P. Langacker, University of Pennsylvania Report No. UPR-0287-T, 1985 (unpublished).

[11]V. Barger, N. G. Deshpande, and K. Whisnant, Phys. Rev. Lett. **56**, 30 (1986).

[12]S. Glashow and S. Weinberg, Phys. Rev. D **15**, 1958 (1977); E. Paschos, *ibid.* **15**, 1966 (1977).

[13]V. Barger and S. Pakvasa, Phys. Lett. **81B**, 195 (1979); V. Barger, W.-Y. Keung, and R. J. N. Phillips, Phys. Rev. D **24**, 1328 (1981).

[14]G. Kane and M. Peskin, Nucl. Phys. **B195**, 29 (1982).

[15]F. J. Gilman and S. H. Rhie, Phys. Rev. D **32**, 324 (1985).

[16]R. Thun, Phys. Lett. **134B**, 459 (1985).

[17]C. Akerlof *et al.*, Phys. Lett. **156B**, 271 (1985); G. J. Feldman *et al.*, Phys. Rev. Lett. **54**, 2289 (1985); W. W. Ash *et al.*, *ibid.* **54**, 2477 (1985).

[18]G. J. Feldman, Report No. SLAC-PUB-3684, 1985 (unpublished).

[19]V. Barger, W.-Y. Keung, and R. J. N. Phillips, Phys. Lett. **141B**, 126 (1984).

[20]G. Arnison *et al.*, Phys. Lett. **147B**, 493 (1984); A. Norton, in Proceedings of the New Particles '85 Conference, Madison, Wisconsin, 1985 (unpublished); C. Rubbia, in *Proceedings of the 1985 International Symposium on Lepton and Photon Interactions at High Energies, Kyoto* (Research Institute for Fundamental Physics, Kyoto University, Kyoto, 1985).

[21]G. Arnison *et al.*, Phys. Lett. **155B**, 442 (1985); K. Eggert, in Proceedings of the New Particles '85 Conference, Madison, Wisconsin, 1985 (unpublished); C. Rubbia (Ref. 20).

[22]G. Arnison *et al.*, Phys. Lett. **139B**, 115 (1984); C. Rubbia (Ref. 20).

[23]V. Barger and R. J. N. Phillips, Phys. Rev. Lett. **55**, 2752 (1985).

[24]D. W. Duke and J. F. Owens, Phys. Rev. D **30**, 49 (1984).

[25]V. Barger, J. Ohnemus, and R. J. N. Phillips (in preparation).

[26]J. R. Cudell, F. Halzen, and K. Hikasa, Phys. Lett. **157B**, 447 (1985); S. D. Ellis, R. Kleiss, and W. J. Stirling, *ibid.* **158B**, 341 (1985); P. Aurenche and R. Kinnunen, Z. Phys. C **28**, 261 (1985).

[27]G. L. Kane, W. W. Repko, and W. B. Rolnick, Phys. Lett. **148B**, 367 (1984).

[28]V. Barger, H. Baer, K. Hagiwara, and R. J. N. Phillips, Phys. Rev. D **30**, 947 (1984).

[29]M. Gronau, C. N. Leung, and J. L. Rosner, Phys. Rev. D **29**, 2539 (1984).